

# The White Dwarf Distance to the Globular Cluster 47 Tucanae and its Age<sup>1</sup>

M. Zoccali<sup>2</sup>, A. Renzini<sup>2</sup>, S. Ortolani<sup>3</sup>, A. Bragaglia<sup>4</sup>, R. Bohlin<sup>5</sup>, E. Carretta<sup>6</sup>, F. R. Ferraro<sup>4</sup>, R. Gilmozzi<sup>2</sup>, J. B. Holberg<sup>7</sup>, G. Marconi<sup>8</sup>, R. M. Rich<sup>9</sup>, F. Wesemael<sup>10</sup>

## ABSTRACT

We present a new determination of the distance (and age) of the Galactic globular cluster 47 Tucanae (NGC 104) based on the fit of its white dwarf (WD) cooling sequence with the empirical fiducial sequence of local WD with known trigonometric parallax, following the method described in Renzini et al. (1996). Both the cluster and the local WDs were imaged with HST+WFPC2 using the same instrument setup. We obtained an apparent distance modulus of  $(m - M)_V = 13.27 \pm 0.14$  consistent with previous ground-based determinations and shorter than that found using *HIPPARCOS* subdwarfs. Coupling our distance determination with a new measure of the apparent magnitude of the main sequence turnoff, based on our HST data, we derive an age of  $13 \pm 2.5$  Gyr.

*Subject headings:*

---

<sup>1</sup>Based on observations with the NASA/ESA *Hubble Space Telescope*, obtained at the Space Telescope Science Institute, which is operated by AURA, Inc., under NASA contract NAS5-26555.

<sup>2</sup>European Southern Observatory, Karl-Schwarzschild 2, D-85748 Garching b. München, Germany; mzoccali@eso.org, arenzini@eso.org, rgilmozz@eso.org

<sup>3</sup>Dipartimento di Astronomia, Università di Padova, vicolo dell'Osservatorio 5, I-35122 – Padova – Italy; ortolani@pd.astro.it

<sup>4</sup>Osservatorio Astronomico, via Ranzani 1, I-40127 Bologna, Italy; angela@bo.astro.it, ferraro@bo.astro.it

<sup>5</sup>Space Telescope Science Institute, 3700 San Martin Drive, Baltimore, Maryland 20771; bohlin@stsci.edu

<sup>6</sup>Osservatorio Astronomico, vicolo dell'Osservatorio 5, I-35122 – Padova – Italy; carretta@pd.astro.it

<sup>7</sup>Lunar and Planetary Laboratory, University of Arizona, Tucson, AZ 85721, USA; holberg@argus.lpl.arizona.edu

<sup>8</sup>Osservatorio Astronomico di Roma, Roma, Italy; gmarconi@eso.org

<sup>9</sup>Department of Physics and Astronomy, Division of Astronomy and Astrophysics, University of California, Los Angeles, CA 90095-1562; rmr@astro.ucla.edu

<sup>10</sup>Département de Physique, Université de Montréal, CP6128, Succ. Centre-Ville, H3C 3J7, Montréal, Québec, Canada; wesemael@astro.umontreal.ca

## 1. Introduction

Galactic globular clusters (GCs) are the oldest systems for which ages can be accurately measured using the stellar evolutionary clock. As such, they constrain the age of the Galaxy, hence of the Universe, and by extension the choice of cosmological parameters. The only observable quantity that can be used to measure the *absolute* age of a GC is the absolute magnitude of the main sequence turnoff ( $M_V^{\text{TO}}$ ). Other observables are also sensitive to age, e.g. the horizontal branch (HB) morphology or the turnoff (TO) colors, but their use is dangerous since in addition to age they are sensitive to other parameters such as mass loss and convective efficiency, respectively.

The TO luminosity of a GC is derived from the observed magnitude of TO stars, correcting for interstellar extinction, and applying the distance modulus. Simple calculations show that the age ( $t$ ) error budget is indeed dominated by the uncertainty in GC distances, with the simple rule  $\delta t/t = \delta \text{mod}$  (Renzini 1991), with e.g., an uncertainty of 0.25 mag in distance modulus implying a  $\sim 25\%$  uncertainty in age. Correspondingly, efforts at improving the accuracy of GC age determinations have focused on the distance issue.

Although the direct measurement of the parallax of several (perhaps all) GCs is on the horizon (SIM, GAIA), for the time being we are still bound to use indirect methods, based on *standard candles*. In most recent years local subdwarfs have been widely used as standard candles, especially after trigonometric parallax data from the *HIPPARCOS* mission have become publicly available.

Indeed, *HIPPARCOS* has produced a large sample of local subdwarfs with accurate parallaxes, and the general perception has been that a sizable reduction of GC ages using the subdwarf method (Reid 1997, 1998; Gratton et al, 1997) was due to the new set of subdwarf parallaxes. Actually, the situation is somewhat more intricate.

For subdwarfs in common with previous, ground-based parallaxes the new *HIPPARCOS* measurements give distance moduli that on average are just 0.1 mag larger (see Fig. 2 in Reid 1997). This corresponds to a reduction in age of only  $\sim 10\%$ , while claimed increases in GC distance moduli were  $\sim 0.3$  mag, and the corresponding reductions over previous age determinations were up to  $\sim 30\%$  (Reid 1997; Gratton et al. 1997). Therefore, *HIPPARCOS* parallaxes alone account for only  $\sim 1/3$  of the claimed reductions, much of the effect coming instead from a variety of cumulative effects, from including subdwarfs and evolved stars with relatively uncertain parallax measurements (Reid 1997), to adopting a different metallicity scale (Gratton et al. 1997). Systematic differences of 1-2 Gyr are also introduced by the use of different theoretical  $M_V^{\text{TO}}$ –age relations. Moreover, contrasting results for M 92 (Pont et al. 1998, Reid 1997 and Carretta et al. 2000) show how much care is required to properly deal with the many observational biases and reddening and metallicity scales. In fact, the fortuitous agreement of the distance moduli derived by Pont et al. and by Carretta et al. is a spurious result, given by adoption of different reddening values and metallicities for the field subdwarfs used in the fitting. In summary, *HIPPARCOS* GC distances and ages still remain matter of debate.

Every method of distance determination presents advantages and disadvantages. For example, GC distances derived from the subdwarf method require the metallicity of the cluster and of each subdwarf to be specified, which makes the method prone to possible systematic biases of the dwarfs vs. giants metallicity scales (see e.g., King et al. 1998). Thus, a mismatch of  $\sim 0.25$  dex in the subdwarfs vs. GC metallicity scales results in a  $\sim 0.25$  mag error in distance and in a 25% error in age (Renzini 1991). For these reasons, we believe that a variety of methods should be used to derive GC distances, as discrepancies among the results should help to identify possible systematic

biases.

As an alternative to the subdwarf method, Renzini et al. (1996, hereafter Paper I) used the DA white dwarf cooling curve as a fiducial to measure the distance to one of the nearest GCs, NGC 6752, obtaining a true modulus of 13.05 mag and an age of 14.5 Gyr (including He diffusion) and 15.5 Gyr (not including He diffusion). In this paper, we use the white dwarf (WD) method to derive the distance modulus to 47 Tuc, a globular cluster that is roughly a factor of ten more metal rich than NGC 6752 ( $[\text{Fe}/\text{H}] = -0.70 \pm 0.03$ ; Carretta & Gratton 1997). In extending our approach to this higher metallicity, we will be able to determine whether there is an age-metallicity relationship among the Galactic GCs. The similarity of the Color-Magnitude diagram (CMD) locus of 47 Tuc to that of bulge globulars NGC 6528 and NGC 6553 (Ortolani et al. 1995) will constrain the ages of bulge clusters of near solar metallicity, as well as of the field population of the Galactic bulge. In principle, the large difference in metallicity between NGC 6752 and 47 Tuc should be useful in giving an independent constraint on the relationship between the  $V$  magnitude of the horizontal branch and  $[\text{Fe}/\text{H}]$ . Unfortunately, the horizontal branch of NGC 6752 is nearly vertical, so its  $V$  magnitude is not so well defined. On the other hand, 47 Tuc has only one peculiar RR-Lyrae star, but does have a well defined red HB at  $V = 14.10$  (Kaluzny et al. 1997). These two clusters were selected for the application of the WD method for being the least reddened ones among the nearest GCs.

## 2. Observations and Data Analysis

A field located 6'5 West of the center of 47 Tuc was observed during Cycle-5 with the HST-WFPC2 camera through the filters F336W, F555W, and F814W. Short exposures with the same instrument setup + long F439W band frames were taken during Cycle-7. Finally, some extra F814W frames of the same field, acquired for astrometric

purposes, were kindly provided by I. King. All in all, the total exposure time was 26300s, 13800, 15880 and 21949 seconds in F336W, F439W, F555W and F814W, respectively. Most of the observations were cosmic-ray split. For the local calibrators, we re-measured the magnitudes of the four DA WDs used in Paper I. In order to achieve a better definition of the local WD sequence, four new local WDs (2 DA + 2 DB) were observed in the same filters. One more star (WD1647+591) was observed but not used because its location in the CMD is too red for its mass ( $0.69 M_{\odot}$ ). We conclude that either it is a binary, or that there must be an error in the mass determination and/or in the parallax.

All the images were de-biased, dark corrected and flatfielded through the standard HST pipeline. Following Silbermann et al. (1996), we have masked out the vignetted region, the saturated and bad pixels and columns using a vignetting mask created by P.B. Stetson, together with the appropriate data quality file for each frame.

### 2.1. Cluster data

The photometric reduction of the frames in the field of 47 Tuc was carried out using the DAOPHOT II/ALLFRAME package (Stetson 1987, 1994). Preliminary photometry was performed on each single frame in order to obtain an approximate list of stars for each of them. The coordinates of the common stars were used for an accurate spatial match among the different frames. With the correct coordinate transformations, we then obtained a single image, which was the median of all the frames, regardless of the filter. In this way we removed all the cosmic rays and obtain the highest signal-to-noise image for star identification. We ran the DAOPHOT/FIND routine on the median image and performed PSF fitting photometry on it, in order to obtain the deepest list of stellar objects, free from spurious detections. Finally, this list was given as input to ALLFRAME, for the simultaneous profile fitting photometry of all the individual frames. The

PSF we used were the WFPC2 reference PSFs extracted by P.B.Stetson (1995) from a large set of uncrowded and unsaturated images.

For a consistent comparison between the 47 Tuc and the local WD stars, all the measured instrumental magnitudes were scaled to a 1s exposure. Aperture corrections for the cluster data were measured from a few isolated stars in each chip and filter. They were applied to the cluster stars in order to convert the PSF magnitudes to the same zero point as the local WDs, measured with an aperture of 0."5 radius. The stars observed with each of the WF chips were then put together, after removing the small chip-to-chip offset (Dolphin 2000).

It is now well known that the WFPC2 detector is affected by a charge transfer efficiency (CTE) problem: a loss of charge during the CCD transfer phase. The amount of the loss depends on the position within the chip, the background counts, and has worsened with time since the installation of the WFPC2 camera. In the last few years various estimates of the size of this effect have been made (e.g., Whitmore & Heyer 1997; Stetson 1998; Whitmore, Heyer & Casertano 1999) that was sometimes mis-interpreted as a “long vs short anomaly” (Casertano & Mutchler 1998). However only very recently Dolphin (2000) provided a formula that takes into account all the dependencies of the charge loss, including its variation with the frame background (and therefore with the exposure time) and its increase with the epoch of the observation. The CTE problem is critical for our method, since it relies mainly on the photometry of faint stars in low background (the background being especially low in the F336W frames). For this reason, we have paid special attention in applying the CTE correction (Dolphin 2000) and in verifying that it gives sound results. The size of the correction for a cluster WD in F336W ranges from a few hundredth up to 0.3 magnitudes, depending on its magnitude and position in the chip. However, the brightest cluster WDs have been corrected

by less than 0.05 mag, and therefore if a residual CTE problem were present, a large difference between the slope of the cluster and the local WD sequence would be present. The fact that no such difference is apparent (Fig. 6) makes us confident about the adopted correction. Finally, a further correction, of the order of a few hundredth of a magnitude, was applied to the F336W magnitudes to account for the time dependence of the UV throughput (Baggett & Gonzaga 1998).

The instrumental CMDs containing the stars from the three WF, in the four color planes, are shown in Fig. 1. The photometry from the PC chip was not used because no WDs were detected in this field. In what follows we will use the notation  $m_{336}$ ,  $m_{439}$ ,  $m_{555}$ ,  $m_{814}$  to indicate the 1s instrumental magnitudes in the F336W, F439W, F555W and F814 filters, respectively. Only the stars detected in  $\geq 50\%$  of the frames in each filter were accepted, and a further selection based on the magnitude errors and the PSF fitting parameters was made. Fig. 1 shows only the stars ( $\sim 2300$ ) in common to the four diagrams, for this reason the main sequence in the  $(m_{555}, m_{555} - m_{814})$  plane is truncated at a magnitude brighter than the  $m_{555}$  limit magnitude. A WD sequence is clearly visible in all four diagrams, although it is better defined in the  $(m_{336}, m_{336} - m_{555})$  and  $(m_{336}, m_{336} - m_{814})$  planes. The main sequence and subgiant branch of the Small Magellanic Cloud old population are also clearly visible at an intermediate location between the 47 Tuc main sequence and the WD sequence. A total of 21 cluster WDs were identified. The WD sequence appears very narrow especially in the two CMDs using the  $m_{336}$  magnitudes, which, due to the larger color baseline, are also the most useful one to distinguish between DA and DB dwarfs (*cf.* Fig. 2). Therefore, we can conclude that only DA WDs have been sampled in this 47 Tuc field, and therefore only the local WDs of the DA type will be used as calibrators for the distance determination.

## 2.2. Local WD data

The local WD calibrators were selected for having a trigonometric parallax with accuracy better than 10% *and* a spectroscopically determined mass as close as possible to  $0.53 M_{\odot}$ , the predicted mass for the globular cluster WDs (Renzini & Fusi Pecci 1988; see also Fig. 1 in Greggio and Renzini 1990).

Every local WD was imaged by each of the 3 WF chips. Aperture photometry was performed within a radius of 0.5 arcsec on each image, the chip-to-chip offset, as determined by Dolphin (2000), was removed, and then the three magnitudes of each star were averaged. The instrumental magnitudes were scaled to 1s exposure and corrected for the decreasing UV throughput ( $m_{336}$  only). The absolute instrumental magnitudes were then obtained by means of the trigonometric parallaxes reported in Table 1. Three of our local calibrating WDs were observed by HIPPARCOS, and their parallaxes, although slightly different from the ground-based ones, do not show any systematic zero point shift. These stars are WD0644+375, WD1327+276, and WD1917-077, and the percent differences ( $\pi_{HIP} - \pi_{VA}$ ) between the parallaxes in the *HIPPARCOS* and the Van Altena et al. (1991) catalog are: +4%, -9%, -12%, respectively. Note that the latter is a DB WD, so it was not used in the fit. In addition, Vauclair et al. (1997) showed that the comparison between the parallaxes the 16 DA WDs in common between the two catalogs reveals no systematic difference.

The Lutz-Kelker correction, calculated according to the formula given in Carretta et al. (2000), amounts to a few hundredth of a magnitudes for all the stars except one, the DB WD WD0002+729, for which it is  $\sim 0.3$  magnitudes. However, this star, being of DB type, was not used for the distance determination. Table 1 also shows that the masses  $M_{WD}$  of a few of the selected local WDs differ appreciably from the ideal value,  $0.53 M_{\odot}$ . In order to obtain a constant-mass sequence ap-

propriate for the match with the cluster WDs, the correction  $\delta(mag) = 2.4(M_{WD} - 0.53)$  as applied to the magnitudes of all the local WDs (Wood 1995; Bergeron, Wesemael & Beauchamp 1995). Moreover, the WD masses listed in Table 1 were all (except WD2326+049) originally derived adopting a WD mass-gravity relation appropriate for WDs without an hydrogen envelope. However, as extensively discussed in Bragaglia, Renzini & Bergeron (1995), there is now general consensus that “evolutionary” values for the mass of the hydrogen envelope should be used, i.e.,  $\sim 10^{-4} M_{\odot}$  for the WD masses of interest here (Napiwotzki, Green & Saffer, 1999). This implies that WD masses in Table 1 were underestimated by  $\sim 0.04 M_{\odot}$  (Bragaglia et al. 1995), and therefore such masses have been increased by this amount in producing the final fiducial WD sequence used in the distance determination. The magnitude correction for each calibrating WD (except WD2326+049 that was obtained with the correct assumption on the envelope thickness) was then taken as  $\delta(mag) = 2.4(M_{WD} + 0.04 - 0.53)$ , where  $M_{WD}$  are the masses in Table 1.

The resulting fiducial WD sequences are shown in Fig. 2, including the best fit straight line in each individual CMD. This plot also shows the size of the Lutz-Kelker (solid vertical lines) and of the mass corrections (dotted lines) applied to each star. Note that the dispersion is very small and that the one reliable DB dwarf is located well outside of the DA sequence only in the ( $m_{336}, m_{336} - m_{555}$ ) plane. As mentioned above, no star in the 47 Tuc CMDs matches the location of the DB sequence. Figure 3 shows the same CMDs but only for the WDs used for the distance determination, with the estimated errors being also indicated.

In summary, the WD fiducial cooling sequence relies on the spectroscopically determined gravities, a theoretical mass-gravity relation corrected for the finite mass of the hydrogen envelope, and on the adopted mass of the cluster WDs,

$0.53 \pm 0.02 M_{\odot}$ . This latter assumption is extensively justified in Paper I, using a series of convergent stellar evolution arguments that we believe are quite solid. Of course, the direct spectroscopic measure of the mass of cluster WDs would be quite reassuring. VLT spectroscopic observations of a sample of four HST selected WDs in the globular cluster NGC 6397 have recently confirmed their nature of WDs of the DA variety (Moehler et al. 2000), although the low S/N of the relatively short exposure spectra of these very faint stars did not allow an accurate determination of the mass.

### 2.3. Photometric zero point check

Globular cluster distance determinations have to rely on standard candles, at least until the direct measure of trigonometric parallaxes will be feasible with SIM/GAIA. The results of the current methods of distance determinations largely rely on the consistency between the observations of the standard candles and their cluster counterparts. Therefore, ideally, the two samples should be measured precisely in the same conditions. However, in most cases this approach is not viable. In the present work, although we observed both the local and the cluster WDs with the same instrument setup, this fact alone does not guarantee the necessary homogeneity, given that we are comparing the photometry from very deep exposures of a sample of extremely faint stars in a crowded field (*i.e.* object for which PSF fitting photometry is needed) with the aperture photometry of a few very bright stars in short-exposure frames of almost empty fields. Therefore, in order to verify that no residual photometric zero point difference can affect our conclusions, we report here the results of some tests we carried out to check the consistency of our measurements, *i.e.*, the linearity of WFPC2 over a range of  $\sim 10$  magnitudes.

The first, most obvious test of the instrumental magnitudes is their calibration to the Landolt system (following Holtzmann et al. 1995 and

Dolphin 2000), and the comparison of the measured calibrated magnitudes with other photometry available in the literature. We emphasize again that we will use only instrumental magnitudes to estimate the distance of 47 Tuc. This test on the calibrated CMD has the sole purpose of checking for the presence of some systematic errors in the instrumental magnitudes, that of course would show up in the calibrated ones. Since no other photometry is available for our field of 47 Tuc, it is possible only to compare our CMD with the fiducial lines of the previous photometry. Fig. 4a shows the comparison between our calibrated  $(V, V - I)$  diagram and the fiducial lines of the photometries by Kaluzny et al. (1997; solid) and Ortolani (private communication; dashed). There appears to be excellent agreement between Ortolani's photometry and this work, while Kaluzny's data seem to be systematically bluer by  $\sim 0.07$  magnitudes. Unfortunately we have no means of establishing which one of the two sets of ground-based photometry is the most correct. Fig. 4b shows the comparison among our  $(V, B - V)$  CMD and the fiducial sequences by Kaluzny et al. (1997; solid) and Hesser et al. (1987, dotted). In this case there is excellent agreement. Figure 4 makes us confident about the zero point of our  $m_{439}$ ,  $m_{555}$  and  $m_{814}$  magnitudes. In particular, the above test is also a check of systematic errors in the aperture corrections, that would affect our distance determination.

We did not calibrate the  $m_{336}$  magnitudes because the F336W filter bandpass differs significantly from the Johnson  $U$ ; and, therefore, the calibration is unreliable, especially for the hottest/coldest stars. However, in order to check the zero point of the  $m_{336}$  instrumental magnitudes, we performed an artificial star test on all the F336W frames. We did this experiments on the F336W frames only because our distance mainly relies on the  $m_{336}$  magnitudes (due to the fact that the WD sequence in this band is less steep, better defined and well sep-

arated from the SMC main sequence) although the F336W S/N for the faintest WDs was not excellent. 100 artificial stars were added, in the same position, on each single frame, with magnitudes in the range of the cluster WDs. Complete DAOPHOTII/ALLFRAME reduction was then carried out on these frames with the same algorithm used for the original images, but manually adding these artificial stars to the star list. The output magnitudes of the artificial stars were then compared with the input ones. Fig. 5 shows this comparison: the systematic error in the output magnitudes is consistent with zero. For this reason we can exclude the possibility of a displacement of the cluster WD sequence in the  $(m_{336}, m_{336} - m_{814})$  or  $(m_{336}, m_{336} - m_{555})$  diagrams, due to the migration of the magnitudes towards brighter values, as a consequence of crowding (Stetson & Harris, 1988). Of course, as all the artificial star tests, this uses model PSFs that could be different from the real ones. Still, the fact that the mean difference between input and output magnitude is consistent with zero gives a good indication that no *significant* migration is present in the  $m_{336}$  photometry of the faint stars. Note that the number of stars in Fig. 5 is not related to the completeness of our photometry because the artificial stars were not identified by the same finding algorithm used for the original ones.

### 3. The distance to 47 Tuc

Once the cooling sequences for the cluster and the local WDs are defined, the distance modulus is the vertical shift that makes the cluster sequence overlap the local one. We adopt a reddening  $E(B - V) = 0.055$ , which is the mean value of those reported by Zinn (1980), Reed et al. (1988) and the Strömgren catalogue (Hauck & Mermilliod 1990). From this value the correspondent interstellar absorption  $A_\lambda$  was derived for the three bands, according to Table 12 in Holtzman et al. (1995), and subtracted them from our magnitudes. Then we shifted the clus-

ter WDs to match the local ones. In doing so, we adopted for the WD sequence in each cluster CMD the same slope determined for the local calibrators, leaving only the zero-point (i.e., the cluster distance modulus) as the adjustable parameter.

Fig. 6 shows the match between the two WD sequences in the three CMDs  $(m_{814}, m_{336} - m_{814})$ ,  $(m_{336}, m_{336} - m_{555})$  and  $(m_{555}, m_{555} - m_{814})$ . The distance modulus required to match the sequences in each panel is shown by the label. The quoted errors are the internal ones, including the magnitude uncertainties both in the local and cluster WDs, and the errors in the adopted parallaxes. The first two panels allow a more accurate distance determination, either because the WD sequence is less steep (left panel), or because of the smaller dispersion around the fiducial sequence (central panel). Note that the scale of both axes has been kept the same in the three panels in order to show the difference in the sequence slopes. The arrow in the lower left corner of each panel shows the *direction* of the reddening vector, whose size has been increased by a factor of three in order to make it more visible. Depending on the difference in slope between the reddening vector and the WD sequence, a fixed uncertainty in the cluster reddening corresponds to a different error in the distance modulus for each panel. In fact, with an uncertainty in the cluster reddening  $\Delta E(B - V) = \pm 0.02$ , the corresponding  $\Delta(m - M)_0$  are  $\mp 0.03$ ,  $\mp 0.01$  and  $\mp 0.07$  in the left, central and right panels of Fig. 6, respectively. The very small variation of the distance modulus derived from the  $(m_{814}, m_{336} - m_{814})$  and the  $(m_{336}, m_{336} - m_{555})$  CMDs is due to the fact that in these planes the WD sequence happens to have a slope very similar to that of the reddening vector (see arrows in Fig. 6). Therefore a change in the adopted reddening shifts the sequence almost parallel to itself. Adding the above quoted systematic uncertainties to the formal errors of the fit, and averaging the three results weighted by the in-

verse of their errors, we obtain a mean distance modulus of  $(m - M)_0 = 13.09 \pm 0.13$ .

A further source of systematic error in this value comes from the adopted mean mass of the cluster WDs:  $M_{WD} = 0.53 \pm 0.02$ . According to the relation quoted above  $\delta(mag) = 2.4(M_{WD} - 0.53)$  an uncertainty of 0.02 in mass implies a 0.05 systematic uncertainty in the distance modulus. Our best estimate for the distance modulus of 47 Tuc is therefore  $(m - M)_0 = 13.09 \pm 0.14$ . Combining this value with the adopted reddening  $E(B - V) = 0.055 \pm 0.02$  and the extinction law  $A_V = 3.2E(B - V)$  the apparent distance modulus is  $(m - M)_V = 13.27 \pm 0.14$ .

In summary, a formula that explicitly shows the dependence of the apparent distance modulus upon the two main assumptions, namely cluster WD masses and reddening, can be expressed as follows:

$$(m - M)_V = 13.09 + 3.2 \times E(B - V) - 2 \times [E(B - V) - 0.055] - 2.4 \times (M_{WD}^{\text{cl}} - 0.53) + 2.4 \times (< M_{WD} > - 0.594)$$

where  $< M_{WD} >$  is the true mean mass of the sample of local WDs, and  $M_{WD}^{\text{cl}}$  the true mass of the cluster WDs, and 0.594 is the mean mass of the sampled local DA WDs given in Table 1, including the correction for the thick hydrogen envelope.

For consistency with Paper I, in our analysis we adopted the trigonometric parallaxes from the Van Altena et al. (1991) catalog. A new version of the same catalog, including some more stars and a new weighting criterion for the various measurements has been released more recently (Van Altena et al. 1995). Due to the new weighting system, the parallaxes of two of the local DA WDs, namely WD0644+729 and WD2126+734, increased by 6% and 9%, corresponding to a decrease of 0.12 and 0.18 magnitudes in their distance modulus, respectively. As a consequence, had we adopted such parallaxes, the distance modulus for 47 Tuc would have *decreased* by  $\sim 0.1$  magnitude.

Table 2 shows a summary of the previous determinations of the distance of 47 Tuc, using a variety of methods, together with the adopted reddening. For a direct comparison among the different distances in Table 2 we reported all to the same reddening  $E(B - V) = 0.055$ , and the result is plotted in Figure 7, with the corresponding errorbars. Our distance determination lies at the lower end of the distribution. It is consistent within the errors with most previous determinations, but it is significantly shorter than the values reported by Reid (1998) and Carretta et al. (2000) using the subdwarf method based on *HIPPARCOS* parallaxes. The cause of this discrepancy remains to be understood.

However, were the correct modulus as high as 13.69, i.e.,  $\sim 0.42$  magnitudes larger than the value indicated by the WD method, then the implied mass of the cluster WDs would be as low as  $0.53 - 0.4/2.4 = 0.36M_{\odot}$ , much less than indicated by stellar evolution theory. Alternatively, the mass of the local WDs (via Balmer line fitting) should have been underestimated by  $\sim 0.17M_{\odot}$ , on average, which also looks quite implausible.

Still assuming that the WD method is to blame, the discrepancy could arise from a mismatch between the cluster and the local WD magnitude scales. As shown by Fig. 6 the distance moduli obtained from the three CMDs differ appreciably one from another. This can only arise from a systematic error in the photometry of at least one of the three bands. Indeed, an error of about  $\Delta m_{555} = +0.05$  would be sufficient to bring the three distance moduli into coincidence, at the value of  $(m - M)_0 = 13.10$  found from the (obviously unvaried)  $(m_{814}, m_{336} - m_{814})$  CMD. Similarly, an error of about  $\Delta m_{814} = -0.08$  would make the three distances coincide with the value of  $(m - M)_0 = 12.95$  found from the middle panel of Fig. 6. Due to the still poorly known CTE correction, the presence of such systematic errors for the very faint cluster WDs cannot be ruled out. However, this would

not help reducing the discrepancy with the subdwarf distances given by Reid (1998) and Carretta et al. (2000). Instead, a systematic error of +0.2 in the  $m_{336}$  magnitudes only would bring the distance moduli derived from the two leftmost panels in Fig. 6 into coincidence with the value of  $(m - M)_0 = 13.34$  found from the  $(m_{555}, m_{555} - m_{814})$  CMD. This would also solve the discrepancy with the Carretta et al. (2000) result. However, it would be more likely that there is a systematic error of the order of 0.05 – 0.08 in the  $V$  and  $I$  instrumental magnitudes, where the WDs are relatively fainter and the field is more crowded, rather than an error as large as 0.2 mag in the  $U$  band.

Finally, it is worth noting that were a residual systematic error the same in *all* the magnitudes, then it would have no effect on the colors, and therefore it would just shift the derived distance moduli by the same amount (equal to the error itself) in all the CMDs.

#### 4. The age of 47 Tuc

The present determination of the distance modulus, combined with the knowledge of the apparent magnitude of the TO and the global metallicity, allows us to derive the age of the cluster, via the turnoff luminosity  $M_V^{\text{TO}}$ . Figure 8 shows the cluster TO region in the CMD constructed using three different color baselines<sup>11</sup>. The horizontal line shows our best estimate of the TO magnitude  $V^{\text{TO}} = 17.65$ , while the two dotted lines define its error range estimate:  $\pm 0.10$  magnitude. Coupled with our distance determination, this gives a TO absolute magnitude  $M_V^{\text{TO}} = 17.65 - 13.27 = 4.38 \pm 0.17$ .

There is little scatter among recent determination of the metallicity of 47 Tuc, and we adopt

$[\text{Fe}/\text{H}] = -0.70$  (Carretta & Gratton 1997). It is now generally believed that for metal poor halo stars and globular clusters the  $\alpha$ -elements enhancement requires values of  $[\alpha/\text{Fe}]$  between 0.4 and 0.6. However, following Gratton, Quarta & Ortolani (1986) we adopt  $[\alpha/\text{Fe}] \approx 0.3$  for the abundance ratios in 47 Tuc.

Figure 9 shows the  $M_V^{\text{TO}}$  vs age relation, for the adopted metallicity  $[\text{M}/\text{H}] = -0.5$ , from the most recent models available in the literature, and the values we derive are listed in Table 3. The first column in Table 3 gives the reference of the adopted model, the second and third give its metallicity and helium abundance, the fourth indicates whether the helium and heavy element diffusion was included in the models, and the next one gives the age corresponding to 47 Tuc. The average age obtained from the models that include atomic diffusion is 12.9 Gyr, while the others give 13.5. As expected (e.g., Castellani et al. 1997) the two values differ by about 0.6 Gyr. Note however that the 1 Gyr discrepancy between the age from Cassisi et al. (1999) and Straniero et al. (1997) is mainly due to the use of a different equation of state in the two sets of models (OPAL the former, and a modified version of the Straniero 1988 the latter; see Cassisi et al. 1999, their Table 1). The age error corresponding to the uncertainty in  $M_V^{\text{TO}}$  is  $\sim 2.2$  Gyr.

The last column of Table 3 shows the ages derived for NGC 6752 assuming  $M_V^{\text{TO}} = 17.4 - 13.27$ . Here  $V^{\text{TO}} = 17.4$  (Penny & Dickens 1986) is the same value adopted in Paper I, while the distance modulus  $(m - M)_V = 13.27$  comes from the value found in Paper I ( $(m - M)_V = 13.17$ ) corrected for the fact that in Paper I a thin hydrogen envelope was assumed for the disk WDs, and therefore a correction of  $2.4 \times 0.04$  is needed (see Sec. 2.2). As Table 1 clearly shows, the two clusters turn out to be coeval within the errors. A forthcoming paper will be devoted to a more direct comparison between the 47 Tuc and NGC 6752 turnoff locations, matching the cluster

<sup>11</sup>Note that, as mentioned above in the text, the calibrated  $U$  magnitude is not reliable at extreme colors because of the large difference between the F336W and the Johnson  $U$  bandpass. We illustrate it here because the relatively narrow width of the main sequence in this plane more clearly indicates the  $V$  magnitude of the turnoff point.

WD sequences .

## 5. Conclusions

The distance of the Galactic globular cluster 47 Tuc has been measured by comparing its WD cooling sequence to the fiducial sequence obtained from a sample of local WDs of known trigonometric parallax. We derive an apparent distance modulus of  $(m - M)_V = 13.27 \pm 0.14$ , or  $(m - M)_0 = 13.09 \pm 0.14$ , implying a turnoff absolute magnitude of  $M_V^{\text{TO}} = 17.65 - 13.27 = 4.38 \pm 0.17$  and therefore an age of  $\sim 13 \pm 2.2$  Gyr, if models including atomic diffusion are used.

We demonstrate again the feasibility of the method using deep optical WFPC2 imaging, that permits very accurate measurement of magnitudes even for stars as faint as the GC WDs. The low dispersion in the cluster cooling sequence together with the fact that the method is not affected by uncertainties in the metallicity, nor in the absolute calibration of the photometry (instrumental magnitude system is consistently used) permit us to measure the distance moduli of the closest clusters with an error of 0.14 mag, which includes systematic uncertainties.

The derived distance modulus is  $\sim 0.42$  mag *shorter* than an extreme value obtained with the subdwarf fitting method. Such “long” distance for 47 Tuc would imply an implausibly low mass for the cluster WDs ( $\sim 0.36 M_{\odot}$ ), or a very large systematic error in the masses of the local WDs as obtained by Balmer-line fitting.

Nevertheless, an important requirement for the application of this method is the linearity of the detector at the two extremes of the dynamical range. HST allows one to obtain very small *statistical* photometric errors down to the faintest stars, but problems like the CTE loss in the WFPC2 may affect the accuracy of the measures. Therefore, the use of the appropriate correction for this effect can be crucial for the result. We applied a state of the art determination of the correction, but identify in the CTE problem the

main possible source of residual systematic bias.

However, to reconcile the “long” distance to 47 Tuc, the mismatch between the cluster and the local WD sequences should be as high as  $\sim 0.36$  mag in U-I, which again we consider highly implausible.

We are deeply grateful to Ivan King for allowing us to measure its proprietary frames from program GO8160. We also thank Peter Stetson for providing us the mask files for vignetting and pixel area correction for WFPC2, and the WFPC2 PSF models that made the data reduction straightforward. We are grateful to Raffaele Gratton for useful discussions.

J.B.H. and R.M.R. wish to acknowledge the support for this work provided by NASA through grant GO 7465 from the Space Telescope Science Institute, which is operated by the Association of Universities for Research in Astronomy, Inc., under NASA contract NAS5-26555.

FRF aknowleges the financial support (MM02241491\_004) of the Ministero della Ricerca Scientifica e Tecnologica to the project *Stellar Observable of Cosmological Relevance*.

## REFERENCES

Baggett, S. & Gonzaga, S. 1998, ISR WFPC2 98-03

Beauchamp, A. 1995, Ph.D. thesis, Univ. Montréal

Bergeron, P., Saffer, R.A., Liebert, J. 1992, ApJ, 394, 228

Bergeron, P., Wesemael, F., Beauchamp, A. 1995, PASP, 107, 1047

Bergeron, P., Wesemael, F., Lamontagne, R., Fontaine, G., Saffer, R.A., Allard, N.F. 1995, ApJ, 449, 258

Bragaglia, A., Bergeron, P. 2000, in preparation

Bragaglia, A., Renzini, A., Bergeron, P. 1995, ApJ, 443, 735

Carretta, E., Gratton, R.G. 1997, A&AS, 121, 95

Carretta, E., Gratton, R.G., Clementini, G., & Fusi Pecci, F. 2000, *ApJ*, 533, 125

Casertano, S., & Mutchler, M. 1998, *Instrument Science Report WFPC2* 98-02

Cassisi, S., Castellani, V., Degl'Innocenti, S., Salaris, M., Weiss, A. 1999, *A&AS*, 134, 103

Castellani, V., Ciacio, F., degl'Innocenti, S., Fiorentini, G. 1997, *A&A*, 332, 801

Dolphin, A.E. 2000, *PASP*, 112, 1397

Ferraro, F.R., Messineo, M., Fusi Pecci, F., de Palo, M.A., Straniero, O., Chieffi, A., Limongi, M. 1999, *AJ*, 118, 1738

Ferraro, F.R., Montegriffo, P., Origlia, L. & Fusi Pecci, F. 2000, *AJ*, 119, 1282

Girardi, L., Bressan, A., Bertelli, G., & Chiosi, C. 2000, *ApJ*, 530, 62

Gratton, R.G., Quarta M.L., & Ortolani S. 1986, *A&A*, 169, 208

Gratton, R.G., Fusi Pecci, F., Carretta, E., Clementini, G., Corsi, C.E., & Lattanzi, M. 1997, *ApJ*, 491, 749

Greggio, L., & Renzini, A., 1990, *ApJ*, 364, 35

Kaluzny, J., Krzeminski, W., Mazur, B., Wysocka, A., Stepień, K. 1997, *Acta Astron.*, 47, 249

Kaluzny, J., Krzeminski, W., Mazur, B., Wysocka, A., Stepień, K. 1998, *Acta Astron.*, 48, 439

King, J.R., Stephens, A., Boesgaard, A.M., Deliyannis, C.P. 1998, *AJ*, 115, 666

Hauck, B., Mermilliod, M. 1990 *A&AS*, 86, 107

Hesser, J.E., Harris, W.E., VandenBerg, D.A., Allwright, J.W.B., Shott, P., Stetson, P.B. 1987 *PASP*, 99, 739

Holtzman, J.A., Burrows, C.J., Casertano, S., Hester, J.J., Trauger, J.T., Watson, A.M. & Worthey, G. 1995, *PASP*, 107, 1065

Moehler, S., Landsman, W.B., & Dorman, B. 2000, *A&A*, 361, 937

Napiwotzki, R., Green, P.J., & Saffer, R.A. 1999, *ApJ*, 517, 399

Ortolani, S., Renzini, A., Gilmozzi, R., Marconi, G., Barbuy, B., Bica, E., Rich, R.M. 1995, *Nature* 377, 701

Oswalt, T.D., et al. 1991, *AJ*, 101, 583

Penny, A.J., & Dickens, R.J. 1986, *MNRAS*, 220, 845

Pont, F., Mayor, M., Turon, C., VandenBerg, D.A. 1998, *A&A*, 329, 87

Reed, B.C., Hesser, J.E., Shawl, S.J. 1988, *PASP*, 100, 545

Reid, I.N. 1997, *AJ*, 114, 161

Reid, I.N. 1998, *AJ*, 115, 204

Renzini, A., Bragaglia, A., Ferraro, F.R., Gilmozzi, R., Ortolani, S., Holberg, J.B., Liebert, J., Wesemael, F., & Bohlin, R.C. 1996 *ApJ*, 465, L23 (PaperI)

Renzini, A., & Fusi Pecci, F. 1988, *ARA&A*, 26, 199

Salaris, M., & Weiss, A., 1998, *A&A*, 335, 943

Salasnich, B., Girardi, L., Weiss, A., & Chiosi, C. 2000, *A&A*, 361, 1023

Silbermann, N. A. et al. 1996, *ApJ*, 470, 1

Stetson, P.B. 1987, *PASP*, 99, 101

Stetson, P.B., & Harris, W.E. 1988, *AJ*, 96, 909

Stetson, P.B. 1995, private communication

Stetson, P.B. 1994, *PASP*, 106, 250

Stetson, P.B. 1998, *PASP*, 110, 1448

Straniero, O. 1988, *A&AS*, 76, 157

Straniero, O., Chieffi, A., Limongi, M. 1997, *ApJ*, 490, 425

Van Altena, W.F., Lee, J.T., Hoffleit, D. 1991, *The General Catalogue of Trigonometric Stellar Parallaxes, Preliminary Version* (New Haven: Yale Univ. Obs.)

Van Altena, W.F., Lee, J.T., Hoffleit, D. 1995, *The General Catalogue of Trigonometric Stellar Parallaxes, Fourth Edition* (New Haven: Yale Univ. Obs.)

VandenBerg, D. A., & Bell, R.A. 1985, ApJS, 58,  
561

VandenBerg, D. A., Swenson, F.J., Rogers, F.J.,  
Iglesias, C.A., Alexander, D.R., 2000, ApJ,  
532, 430

Vauclair, G., Schmidt, H., Koester, D., & Allard,  
N. 1997, A&A, 325, 1055

Whitmore, B., and Heyer, M. 1997, Instrument  
Science Report WFPC2 97-08

Whitmore, B., Heyer, I., & Casertano, S. 1999,  
PASP, 111, 1559

Wood, M.A. 1995, in White Dwarfs, ed. D.  
Koester & K. Werner (Berlin: Springer), 41

Zinn, R. 1980, ApJS, 42, 19

TABLE 1  
THE LOCAL CALIBRATING WHITE DWARFS

WD	$\pi \pm \Delta\pi$	Ref.	$M \pm \Delta M$	Ref.	WD type
WD0002+729	$0.0291 \pm 0.0047$	1	$0.600 \pm 0.030$	2	DB
WD0644+375	$0.0626 \pm 0.0018$	1	$0.655 \pm 0.020$	3	DA
WD1327-083	$0.0611 \pm 0.0028$	1	$0.502 \pm 0.017$	4	DA
WD1917-077	$0.1010 \pm 0.0026$	1	$0.550 \pm 0.050$	5	DB
WD1935+327	$0.0561 \pm 0.0029$	1	$0.512 \pm 0.013$	6	DA
WD2126+734	$0.0433 \pm 0.0035$	1	$0.513 \pm 0.012$	6	DA
WD2326+049	$0.0725 \pm 0.0048$	1	$0.690 \pm 0.025$	7	DA
WD2341+322	$0.0559 \pm 0.0017$	1	$0.494 \pm 0.021$	6	DA

References: (1) Van Altena et al. (1991); (2) Beauchamp (1995); (3) Bergeron, Saffer & Liebert (1992); (4) Bragaglia et al. (1995); (5) Oswalt et al. (1991); (6) Bragaglia & Bergeron (2000); (7) Bergeron et al. (1995)

TABLE 2  
47 TUC DISTANCE DETERMINATIONS

Method	$(m - M)_V$	$E(B - V)$	Reference
HB fitting	$13.40 \pm 0.20$	0.040	Hesser et al. (1987)
Baade-Wesselink	$13.36 \pm 0.17$	0.040	Storm et al. (1994)
HB fitting	$13.45 \pm 0.07$	0.040	Kaluzny et al. (1998)
HB fitting	$13.50 \pm 0.05$	0.050	Salaris & Weiss (1998)
HB fitting	$13.43 \pm 0.15$	0.040	Ferraro et al. (1999)
RGB tip	$13.42 \pm 0.20$	0.040	Ferraro et al. (2000)
MS fitting	$13.69 \pm 0.15$	0.040	Reid (1998)
MS fitting	$13.55 \pm 0.09$	0.055	Carretta et al (2000)
WDs	$13.27 \pm 0.14$	0.055	This work

TABLE 3  
THE AGE OF 47 TUC USING DIFFERENT MODELS

Model	[M/H]	Y	diffusion	age (Gyr)	NGC 6752 age
Straniero et al. (1997)	-0.60	0.230	yes	13.5	13.0
Cassisi et al. (1999)	-0.52	0.230	yes	12.4	11.7
VandenBerg et al. (2000)	-0.62	0.241	no	13.7	13.3
Girardi et al. (2000)	-0.50	0.245	no	13.3	13.5
Salasnich et al. (2000)	-0.50	0.245	yes	12.8	

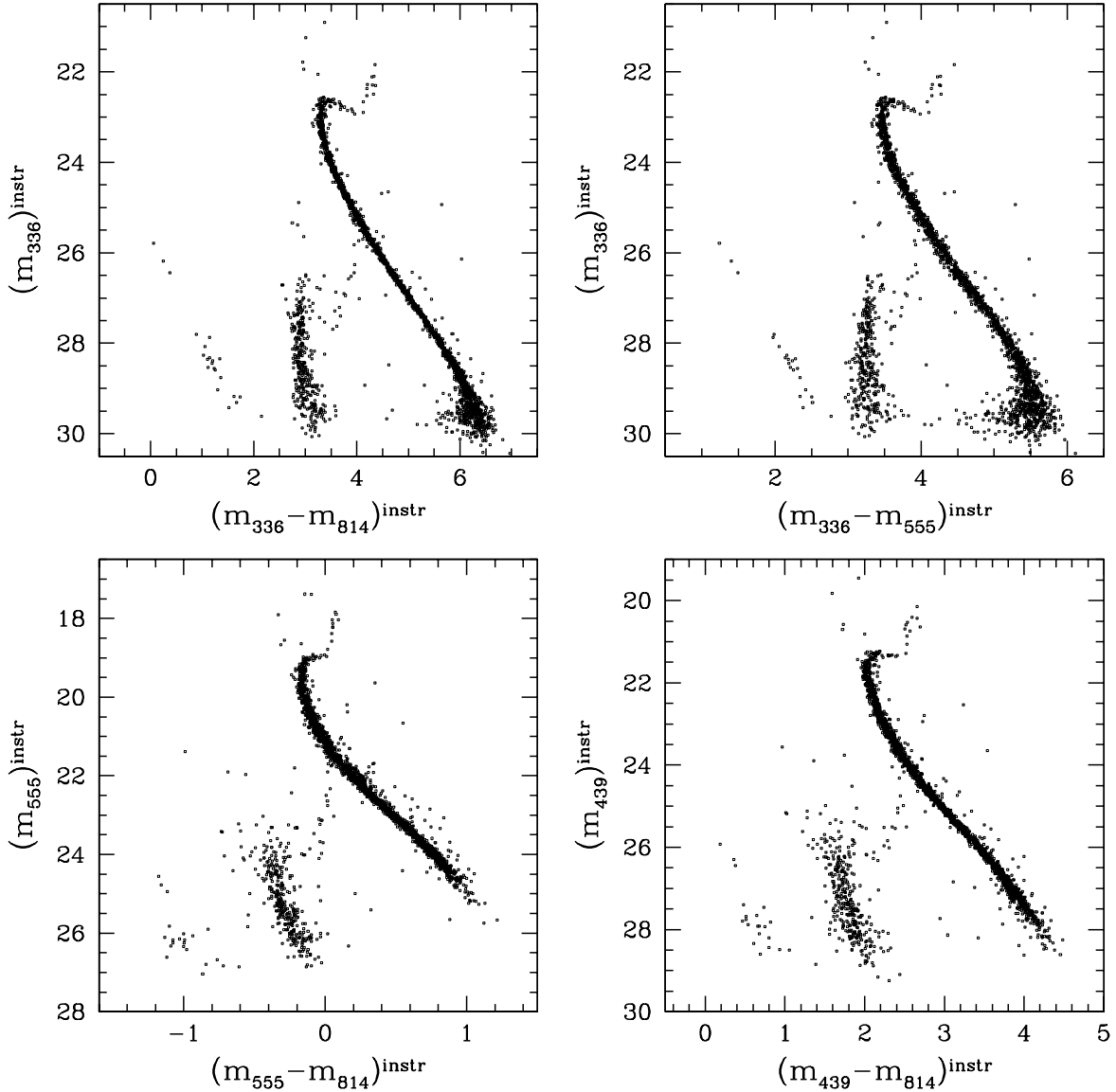


Fig. 1.— The instrumental CMD of the observed 47 Tuc field. Three main branches are clearly distinguishable: the cluster MS on the right, the SMC MS and SGB in the middle, and the cluster white dwarf sequence on the left.

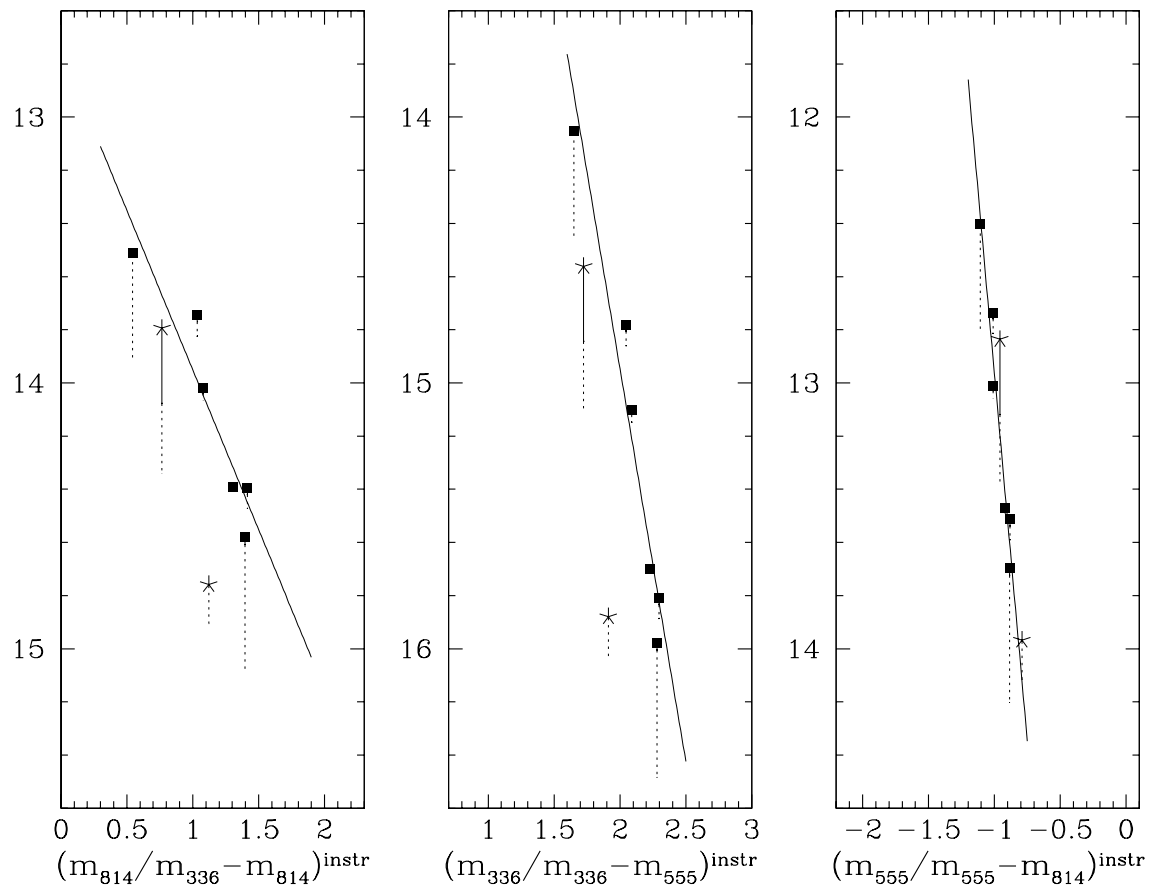


Fig. 2.— Instrumental CMDs of the local WDs used as calibrators. DA WDs are plotted as filled squares, DBs are the asterisks. A least square fit to the DA WDs is shown as a solid line. The vertical dotted lines show the size of the magnitude correction applied to the WDs whose masses differ from 0.53, while the solid vertical line is the size of the Lutz-Kelker correction.

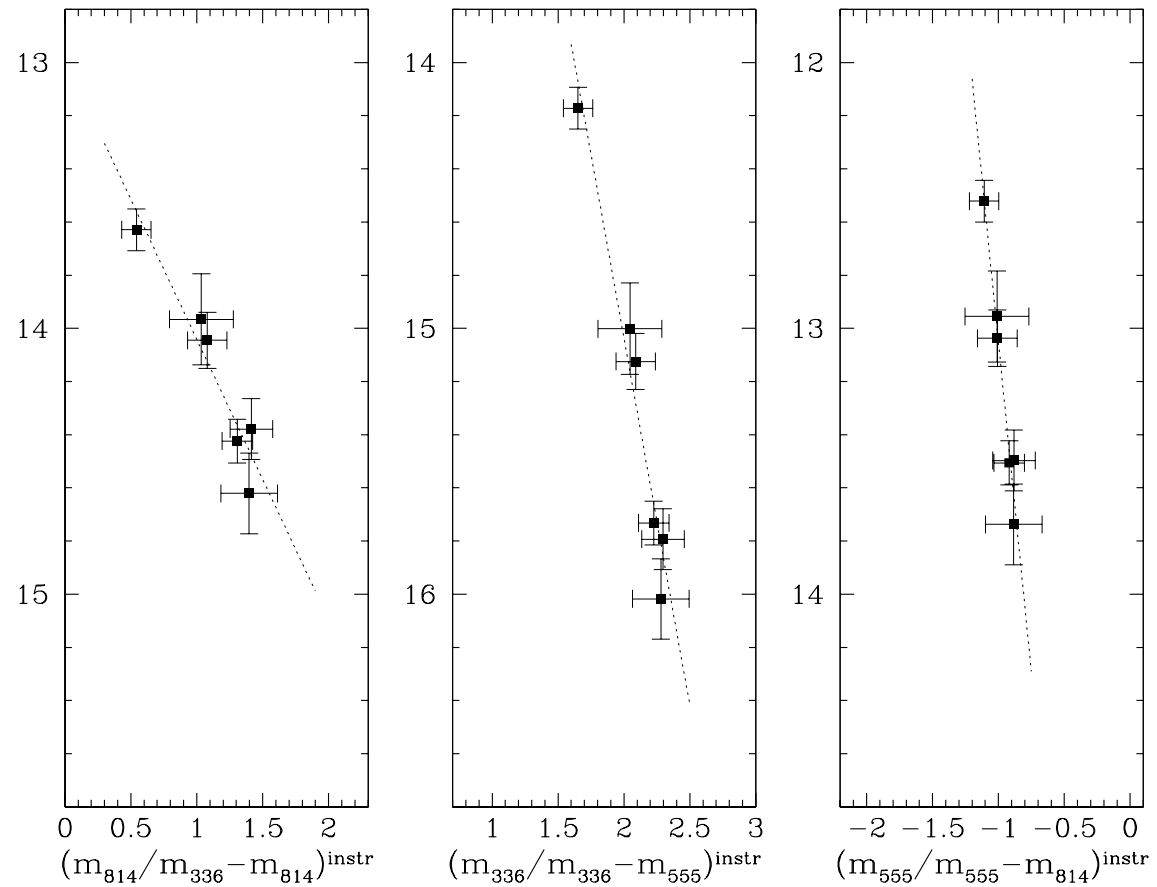


Fig. 3.— Same as Fig. 2, but only for the DA WDs and with errorbars. The latter include the internal photometric errors, as well as the uncertainties in the parallax and mass determinations listed in Table 1.

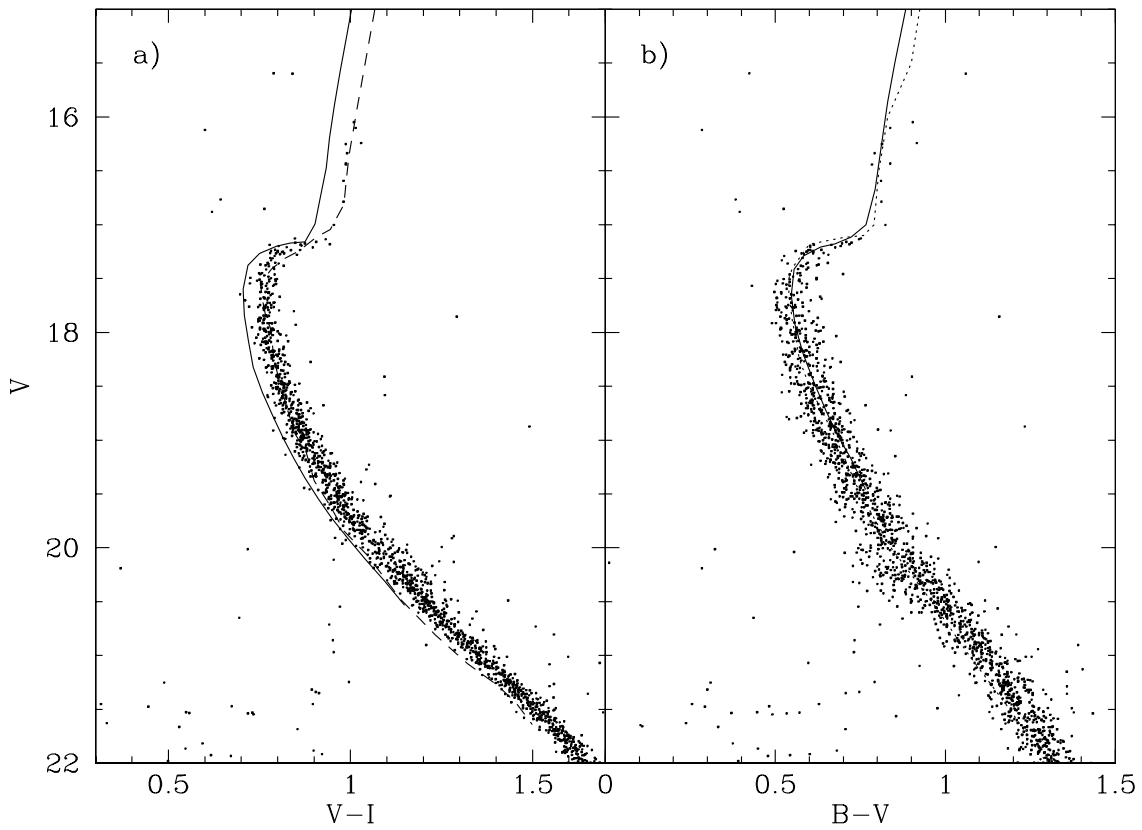


Fig. 4.— Comparison between our calibrated data and the fiducial lines of previously published photometries. Left panel:  $V$ ,  $V-I$  CMD compared with the fiducial lines from Kaluzny et al. (1997; solid) and Ortolani 2000 (dashed). Right panel:  $B$ ,  $B-V$  CMD compared with Kaluzny et al. (1997; solid), and Hesser et al. (1987; dotted).

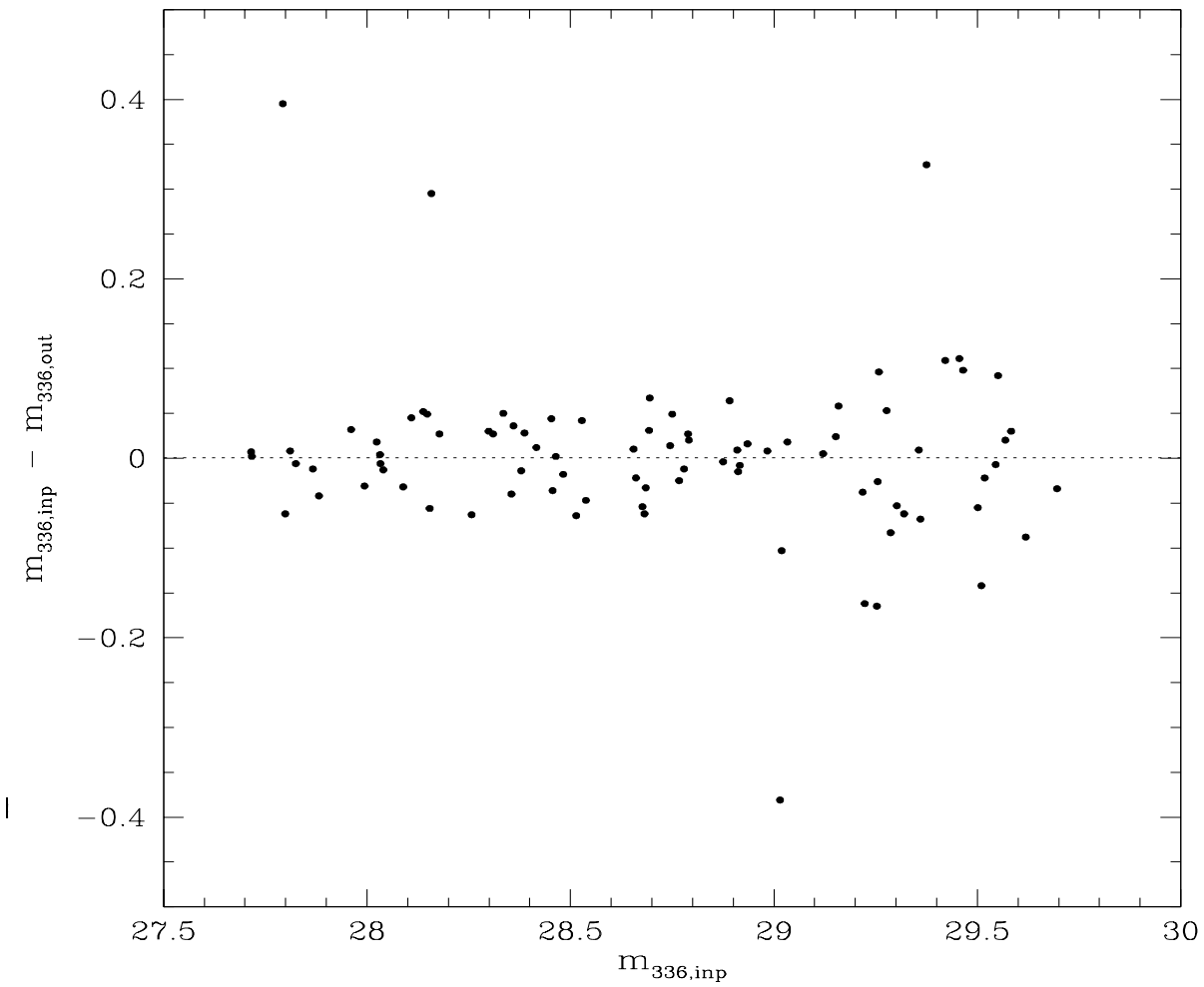


Fig. 5.— Artificial star test in the F336W band. The difference between the input and output magnitudes are plotted as a function of the input magnitude.

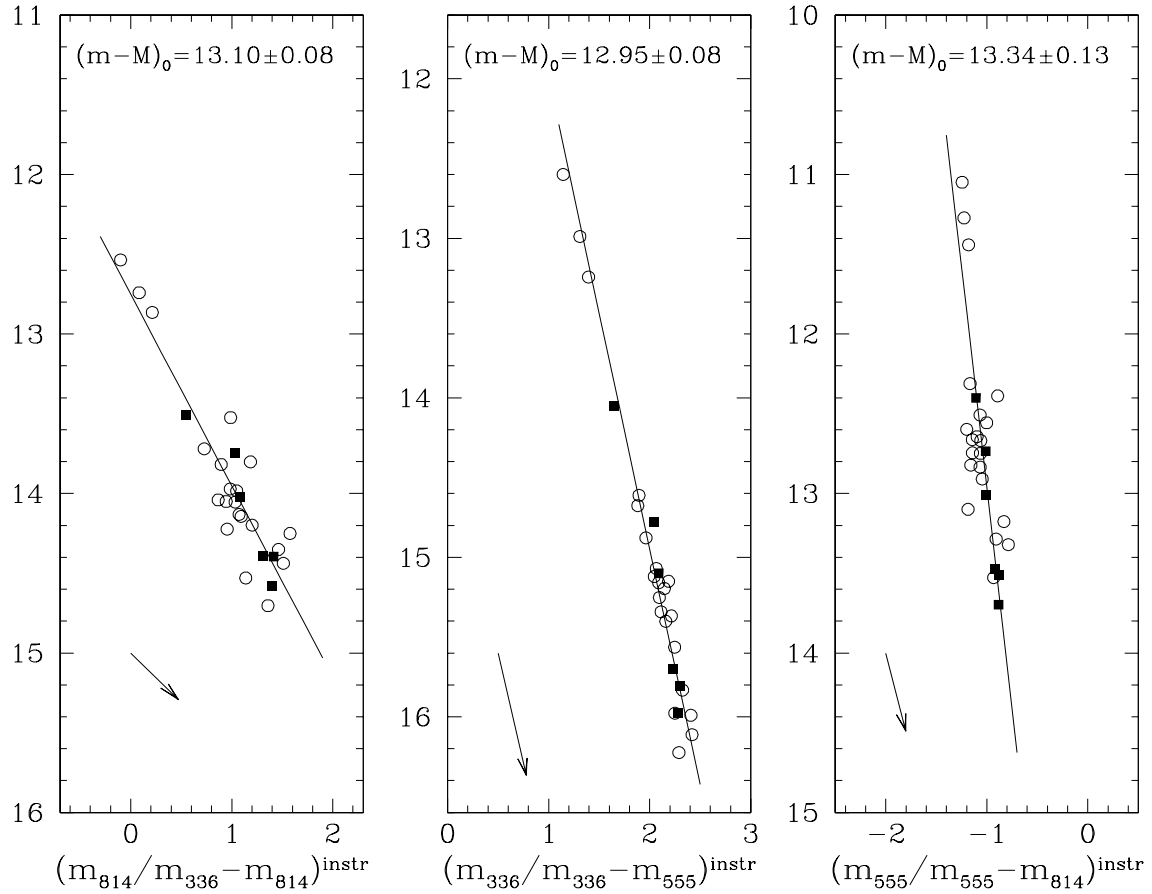


Fig. 6.— Match between the 21 WDs identified in 47 Tuc (open circles) and the local DA WDs (filled squares). The distance moduli required to match the two sequences in the three planes are shown in the labels, together with their formal error. The arrow on the lower left corner shows the direction of the reddening vector, whose size has been increased by a factor of three in order to make it more visible. The dotted line in the central and right panel shows the displacement of the cluster WD sequence if the mean distance modulus were adopted.

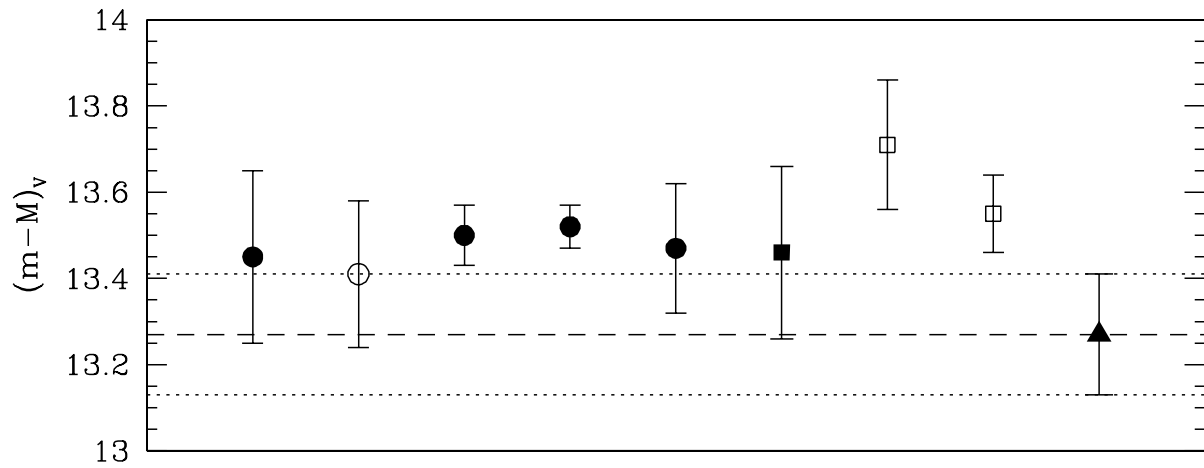


Fig. 7.— Determinations of the distance of 47 Tuc by different authors, in the same order as Table 2, from left to right. Different symbols refer to different methods: HB fitting (filled circles), the unique RR-Lyrae variable (open circle), RGB tip (filled square), subdwarf fitting (open squares) and this work (filled triangle).

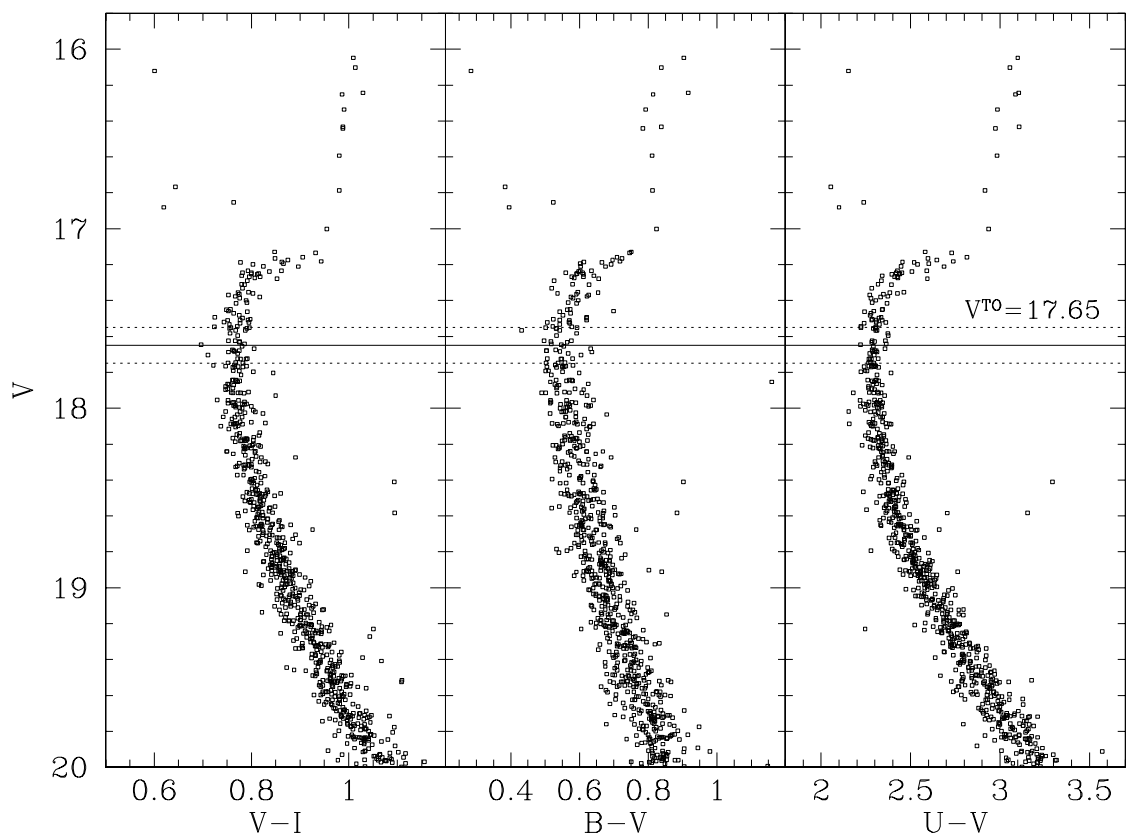


Fig. 8.— The turnoff region in the calibrated CMD.

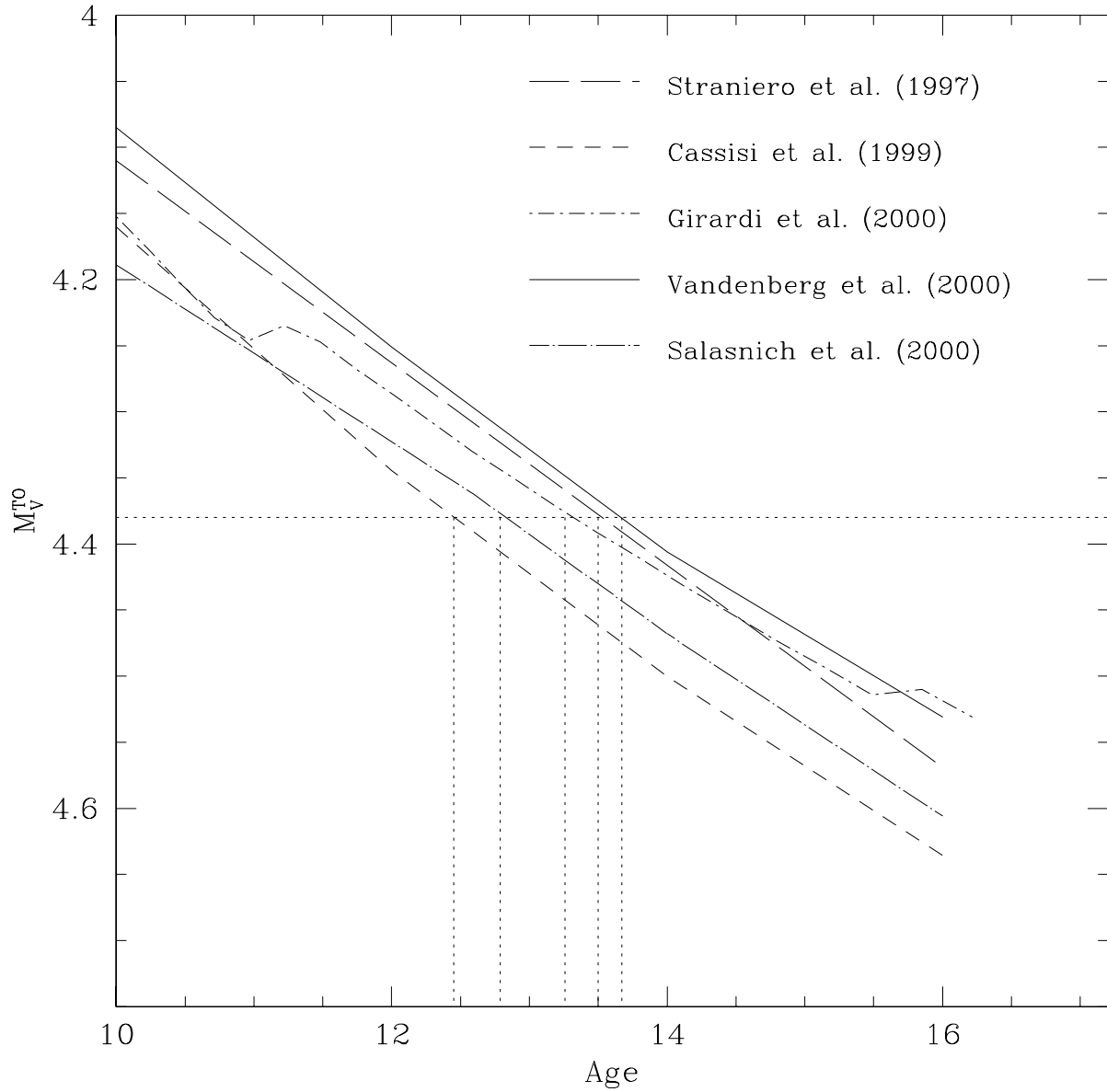


Fig. 9.—  $M_V^{\text{TO}}$  vs age relation derived from different theoretical models. The horizontal dotted line shows the estimated location of  $M_V^{\text{TO}}$  for 47 Tuc, and the vertical ones the corresponding ages, according to the three models.